

# Overview of Radio Coronal Magnetography

# OUTLINE (PART 1)

The uses and abuses of various emission mechanisms

- ✘ Thermal free-free radiation
- ✘ Thermal gyroresonance radiation (SW)
- ✘ Nonthermal gyrosynchrotron radiation
- ✘ Radio bursts

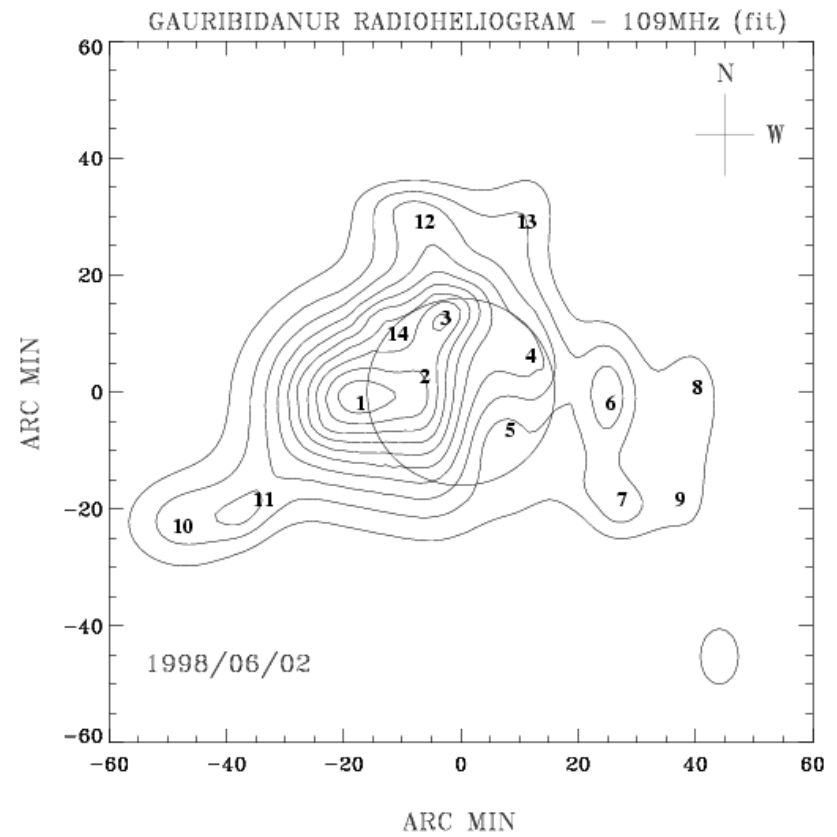
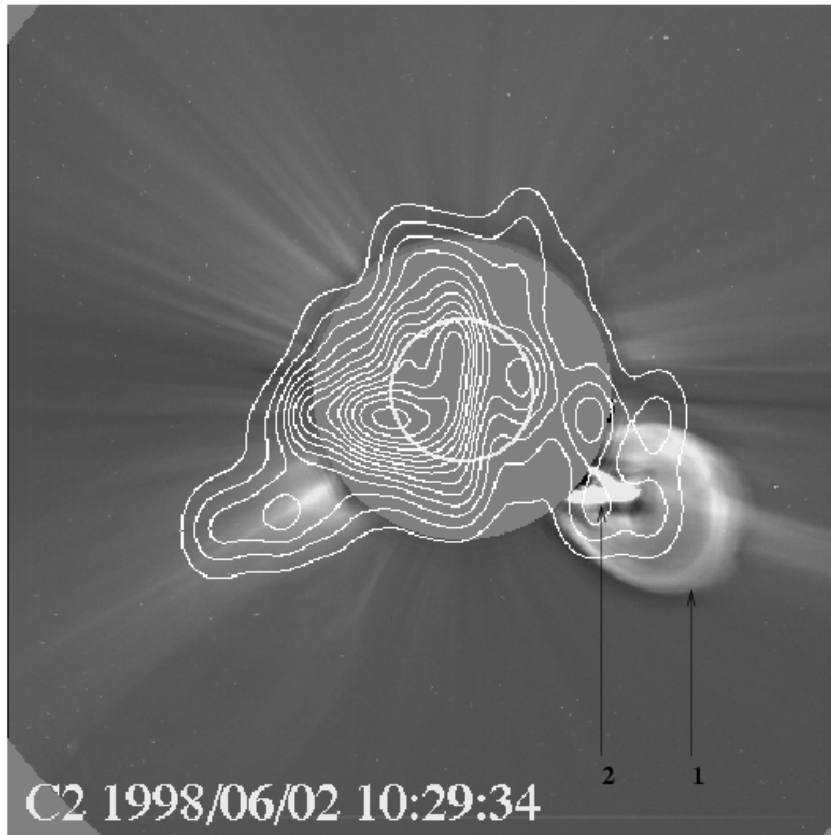
# OUTLINE (PART 2)

Propagation phenomena and related

- ✘ Ray tracing
- ✘ Scattering phenomena
- ✘ Faraday rotation
- ✘ QT propagation

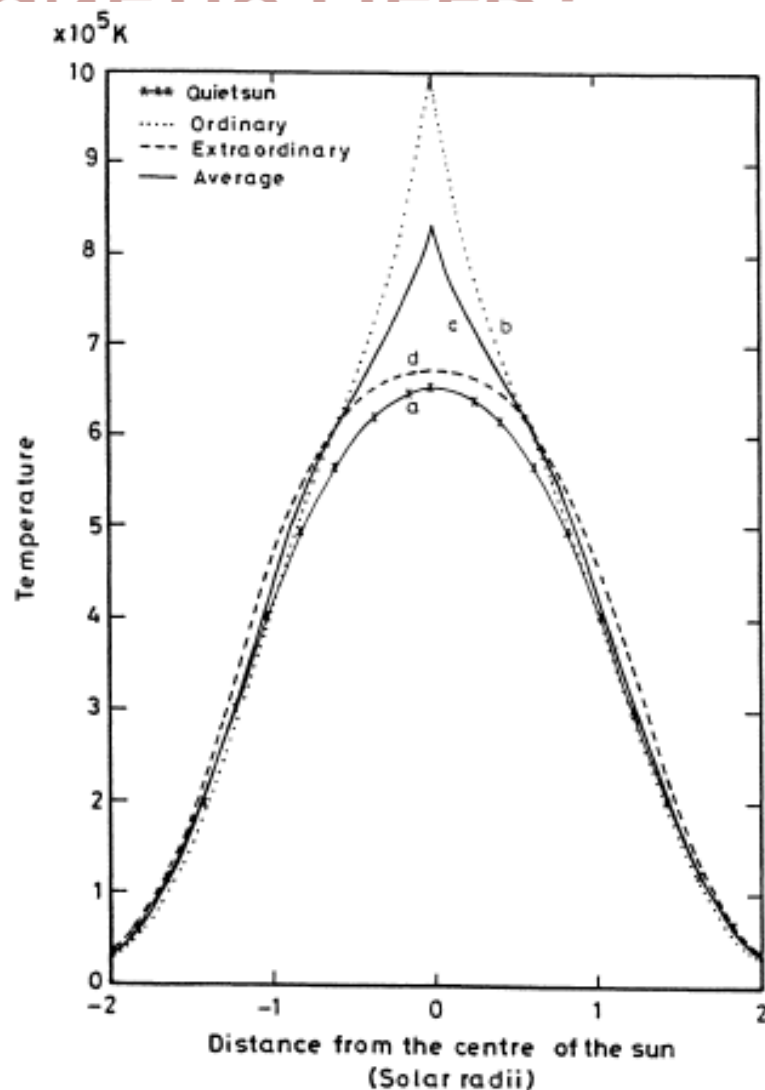


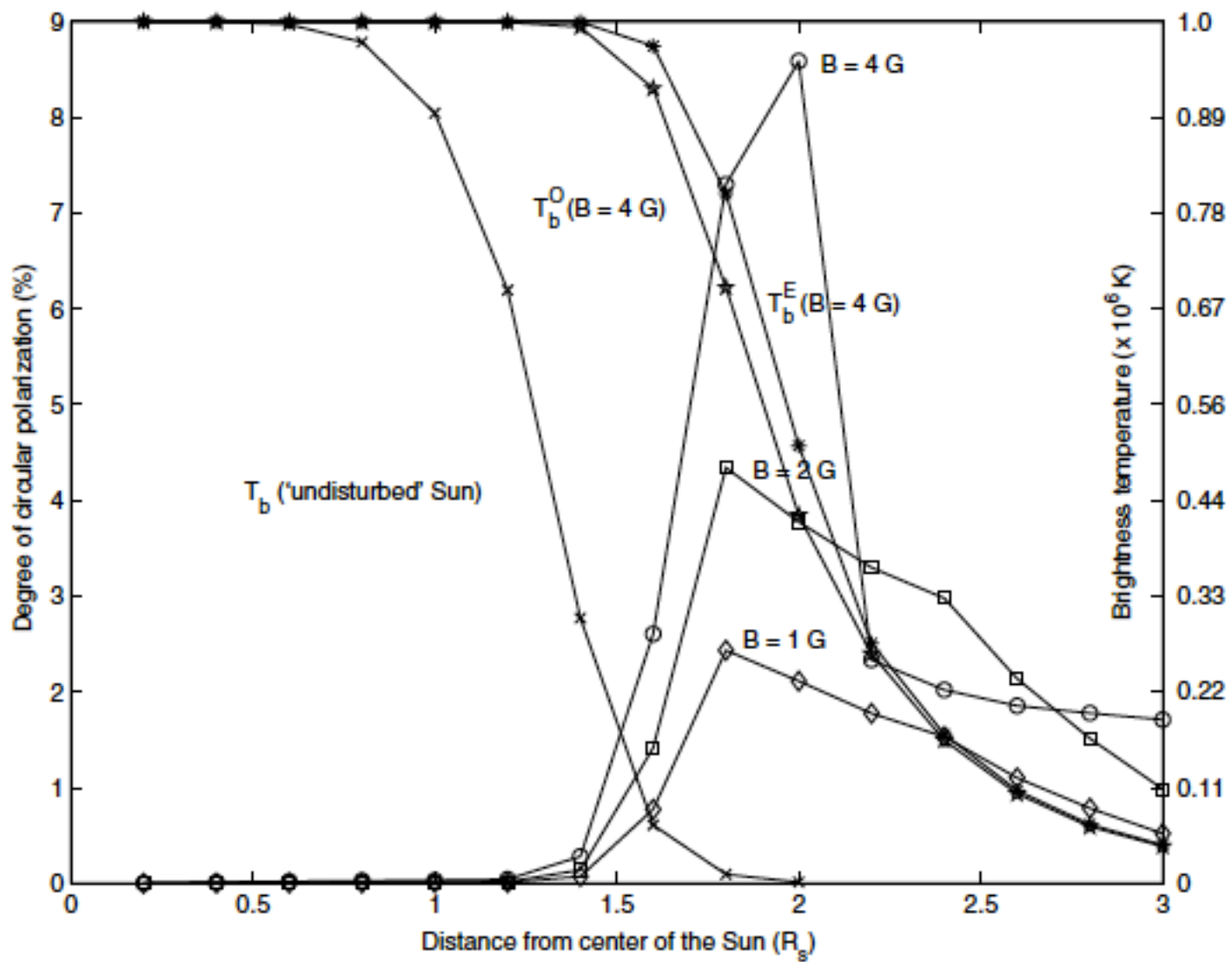
## Gauribindanur RH: 109 MHz



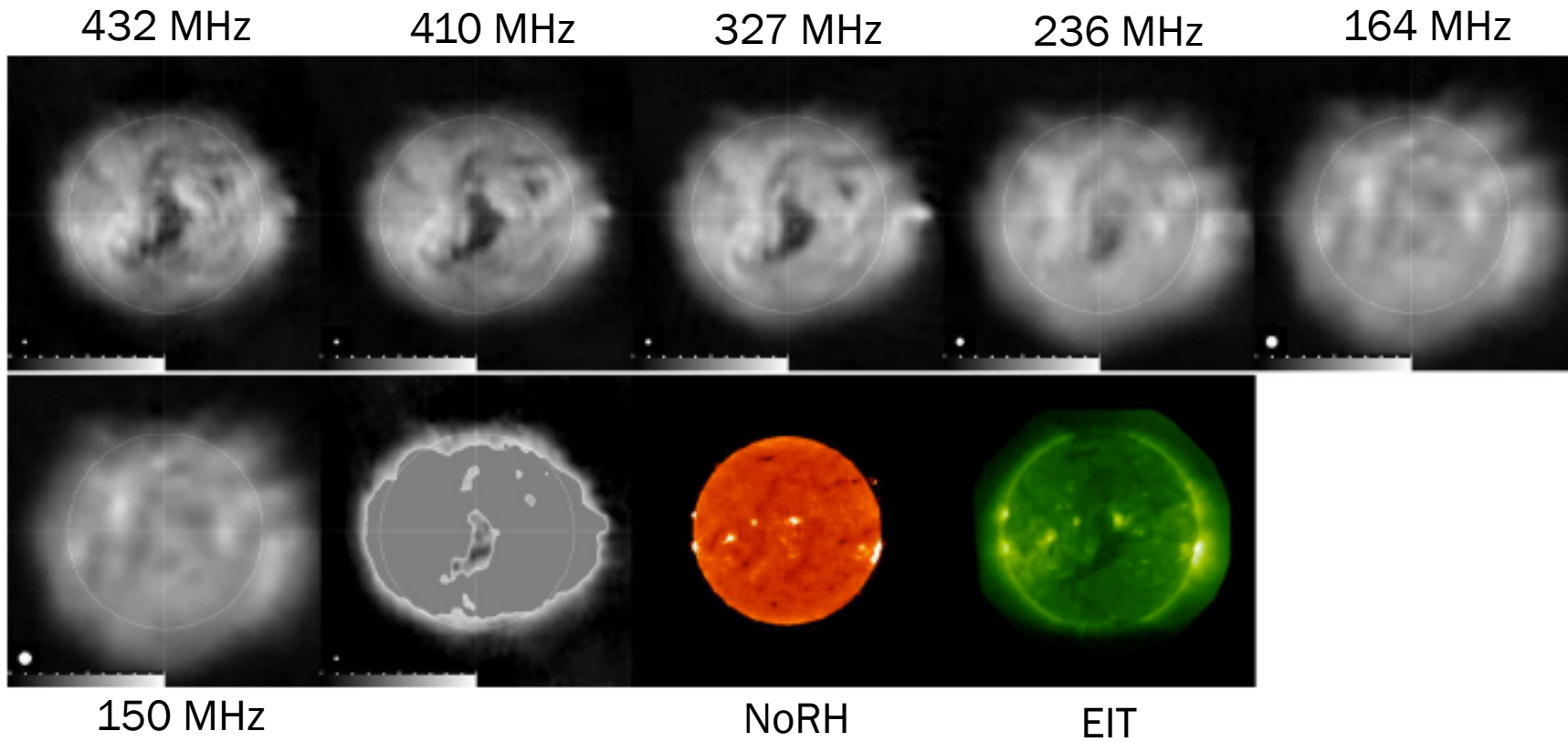
# WHAT ABOUT THE MAGNETIC FIELD?

- ✘ Surprisingly little work has been done with ray-tracing codes to model the magnetized corona
- ✘ Golap & Sastry (1994) used **Haselgrove's Equations** (1955) to compute the radio brightness distribution of the Sun at 35 MHz in the presence of a radial magnetic field (DM78)
- ✘ Sastry (2009) subsequently explored streamer and CH structures, again using a radial field
- ✘ An area ripe for development!





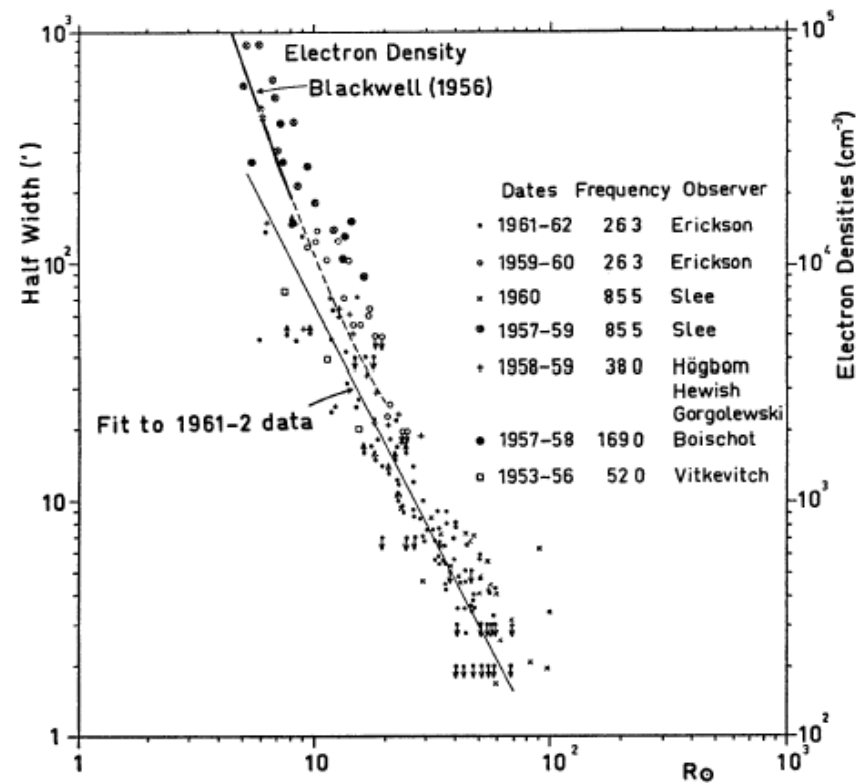
# NRH: 2004 June 27





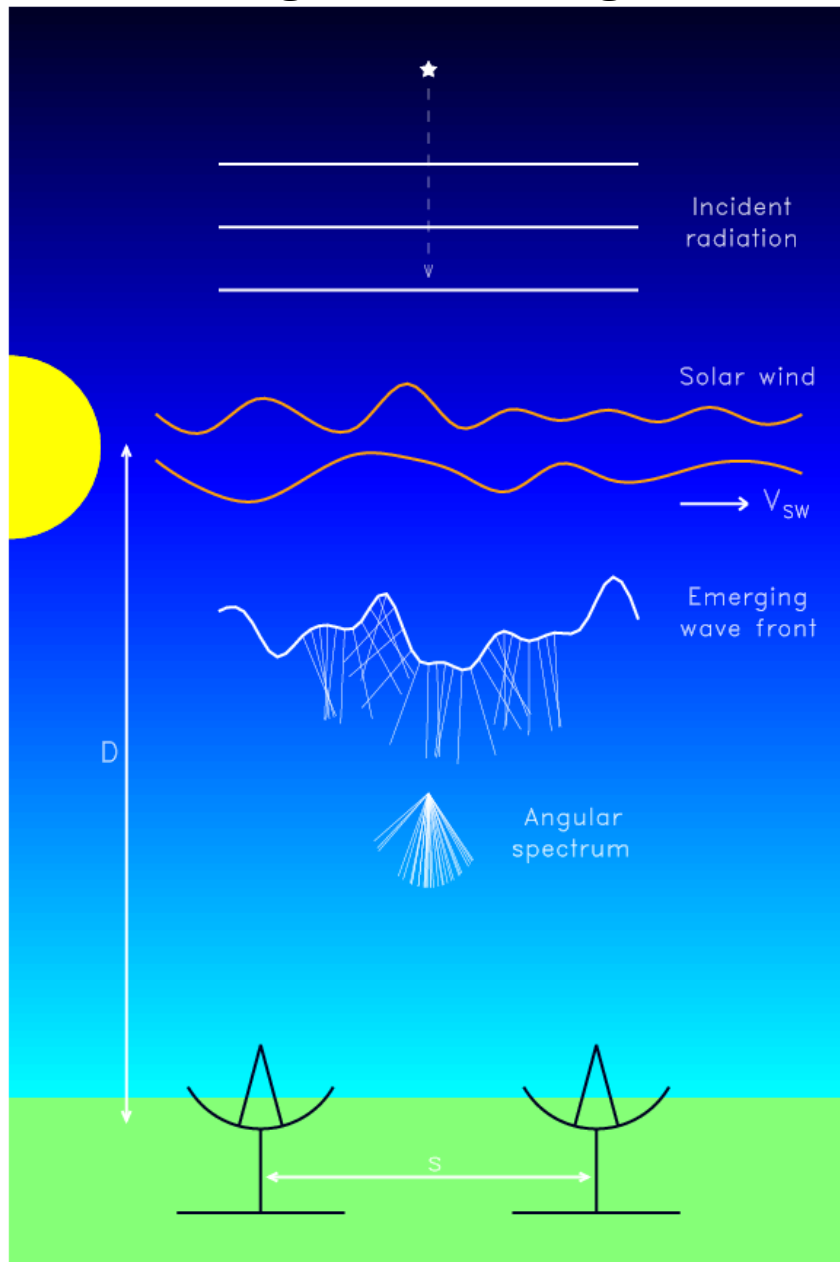
# CORONAL SCATTERING

- ✘ Seminal work by Högbom (1959), Fokker (1965), Steinberg et al. (1971)
- ✘ Motivated by observations of:
  - + Radio bursts a wavelengths
    - $\lambda > 1\text{m}$ :
    - ✘ angular size
    - ✘ polarization
    - ✘ center-to-limb variation
- ✘ Angular broadening of cosmic sources viewed through the outer corona

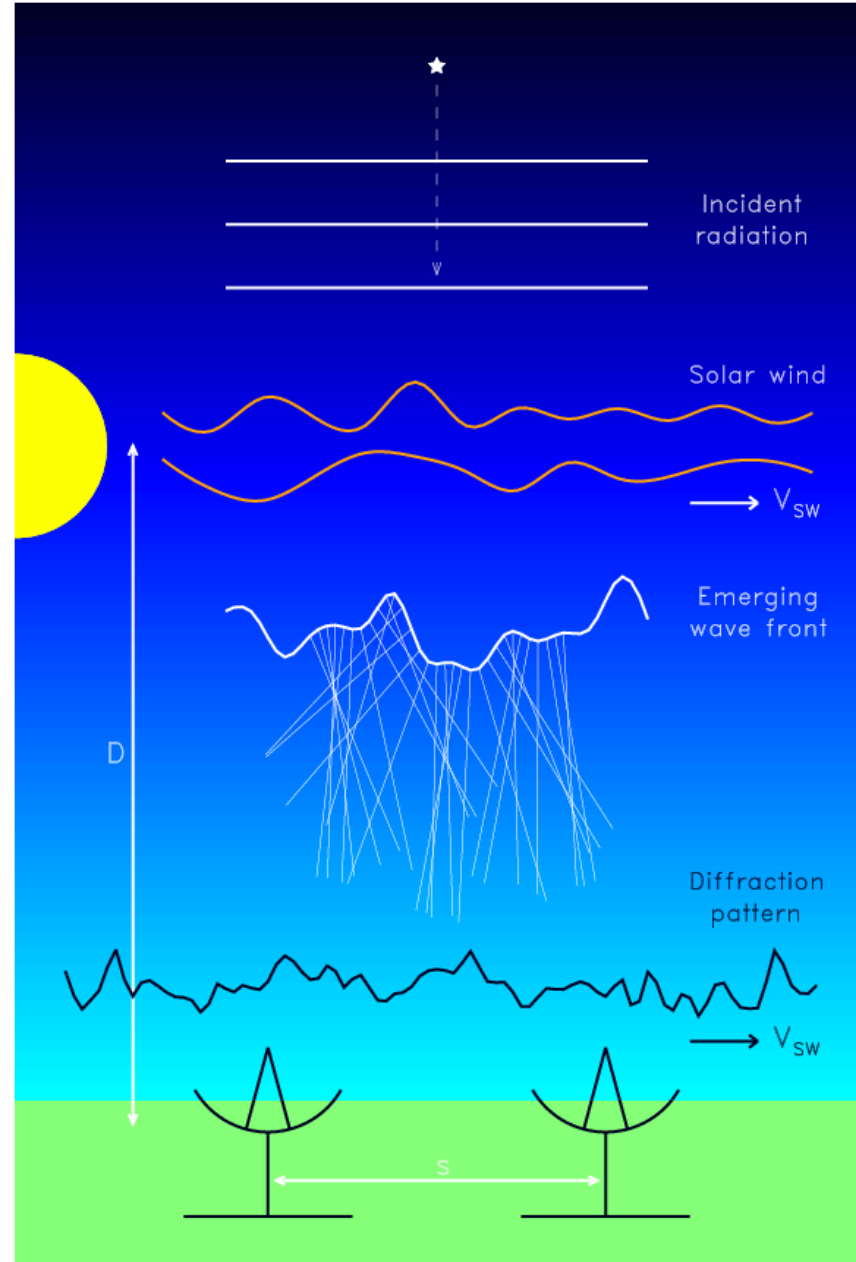


Erickson 1964

## Angular broadening



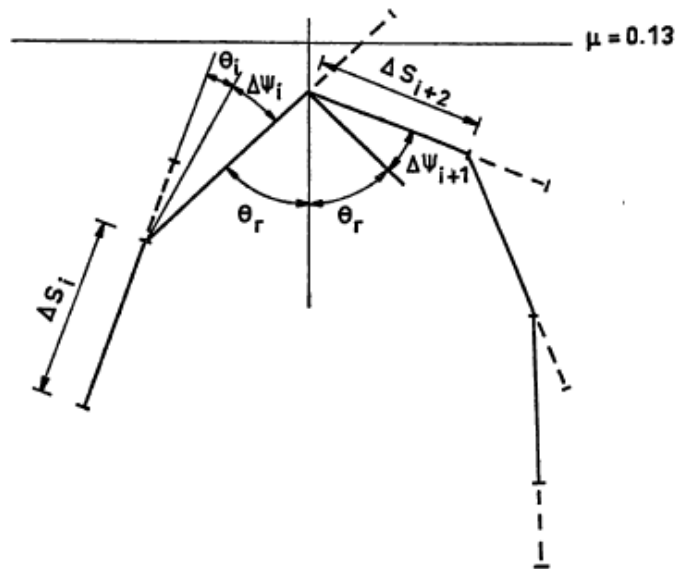
## Scintillations



# CORONAL SCATTERING

- ✘ Steinberg et al. (1971) performed ray-tracing calculations in a Newkirk corona with density inhomogeneities described by a Gaussian correlation function:

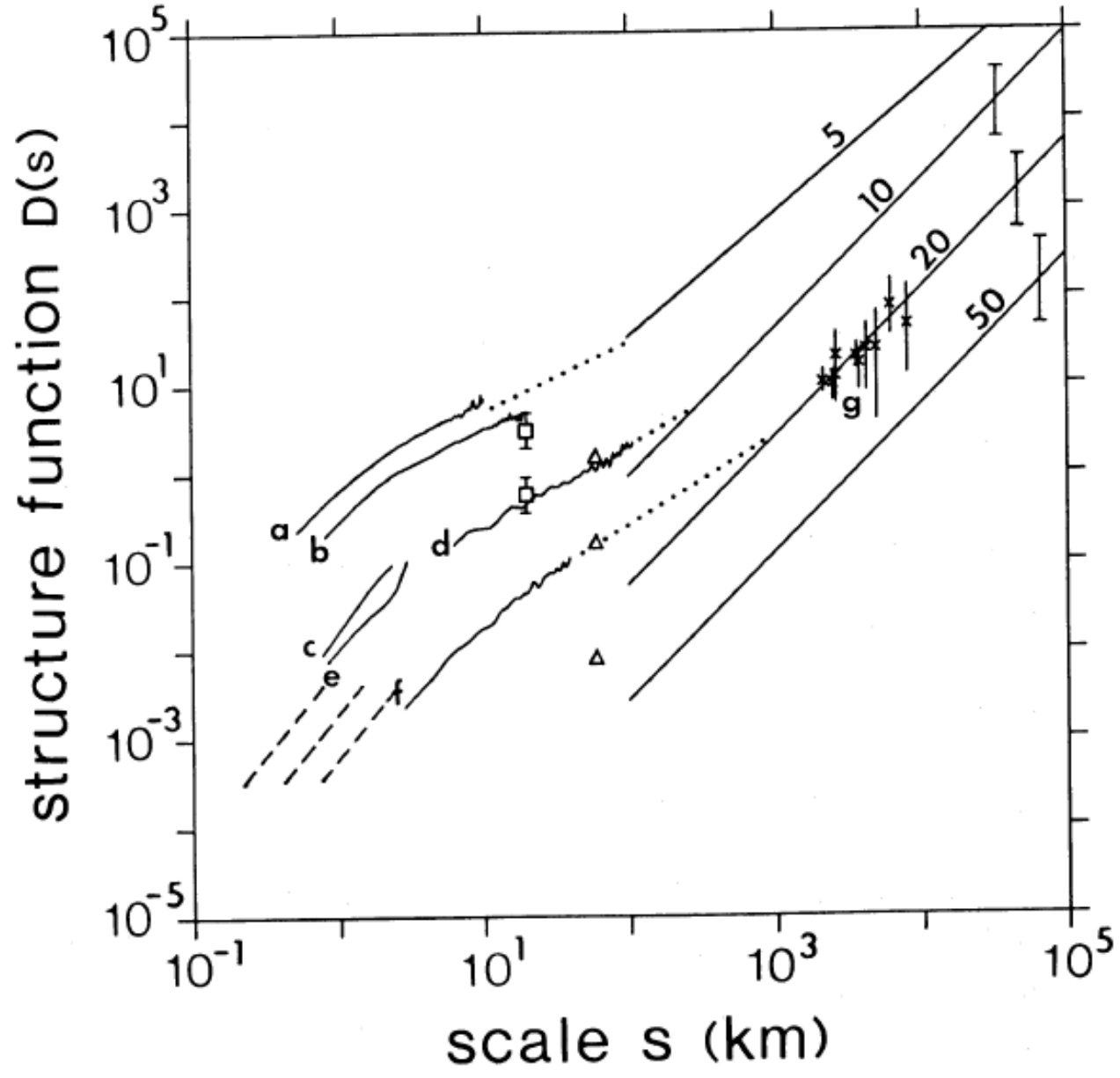
$$\langle \delta\mu(r_1)\delta\mu(r_2) \rangle = \langle -\delta\mu^2 \rangle \exp\left[-\frac{|r_1 - r_2|^2}{h^2}\right] \quad h \ll \rho$$



$$\langle \delta\Psi^2 \rangle = \langle \delta\Omega^2 \rangle = 2\pi^{1/2} \int_{ray} \frac{\langle \delta\mu^2 \rangle}{\mu^2 h} dS$$

Concluded large scale refraction and scattering play a significant role in the propagation of radio waves in the corona.





Coles & Harmon 1989

# SCATTERING AT CM AND DM WAVELENGTHS

- ✘ Ignore large scale refraction
- ✘ An interferometric array measure the mutual coherence function of the electric field

$$\Gamma(s) = \frac{\langle E(\mathbf{r})E^*(\mathbf{r} + \mathbf{s}) \rangle}{\langle |E|^2 \rangle}$$

- ✘ It is related to the *wave structure function*  $D(s)$  through

$$\Gamma(s) = \exp [-D(s)/2]$$

where  $D(s) = \langle [\phi(\mathbf{r}) - \phi(\mathbf{r} + \mathbf{s})]^2 \rangle$  and  $\phi(\mathbf{r}) = r_e \lambda \int n(\mathbf{r}) dz$

- ✘ The spatial spectrum of electron density fluctuations  $\Phi_n(\kappa)$  is the Fourier transform of the spatial correlation function of the electron density fluctuations.

# SCATTERING AT CM AND DM WAVELENGTHS

For a spatial spectrum  $\Phi_n(\kappa) = C_n^2 \kappa^{-\alpha-2} \exp [-(\kappa l_0/2)^2]$  we have

$$\frac{\partial D(s, z)}{\partial z} = \frac{8\pi^2}{\alpha} \Gamma\left(1 - \frac{\alpha}{2}\right) C_n^2(z) r_e^2 \lambda^2 \left(\frac{l_0}{2}\right)^\alpha \times \left\{ {}_1F_1\left[-\frac{\alpha}{2}, 1, -\left(\frac{s}{l_0}\right)^2\right] - 1 \right\}$$

In the limit that  $s \ll l_0$ , this becomes

$$\frac{\partial D(s, z)}{\partial z} = \frac{4\pi^2}{2^\alpha} \Gamma\left(1 - \frac{\alpha}{2}\right) C_n^2(z) r_e^2 \lambda^2 l_0^{\alpha-2} s^2 \quad (s \ll l_0)$$

Which is true for spherical wave propagation:

$$D(s) = \int_0^L \frac{\partial D(s, z)}{\partial z} dz \quad \longrightarrow \quad D(s) = \int_0^L \frac{\partial D(sz/L, z)}{\partial z} dz$$

# SCATTERING AT CM AND DM WAVELENGTHS

Returning to the mutual coherence function it's seen that the angular width of a point source can be characterized by the scale  $s_0$  where  $D(s_0)=1$  so that  $\theta_c = (ks_0)^{-1}$  and  $\theta_G = 2.35\theta_c$ .

$$\Gamma(\mathbf{s}) = \exp [-D(\mathbf{s})/2]$$

When observing an extended source in the absence of turbulence we have

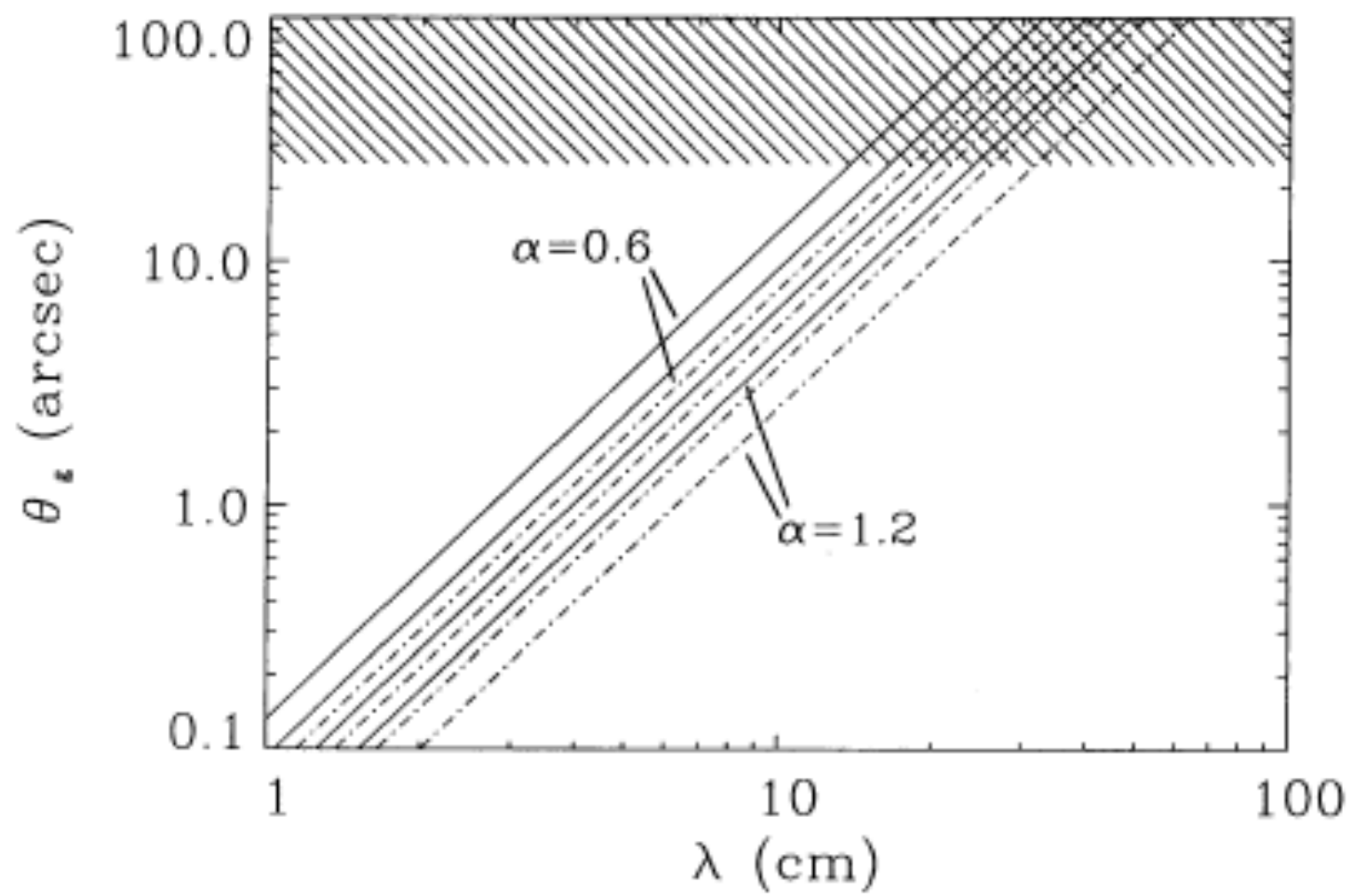
$$\Gamma(\mathbf{s}) = V(\mathbf{s})$$

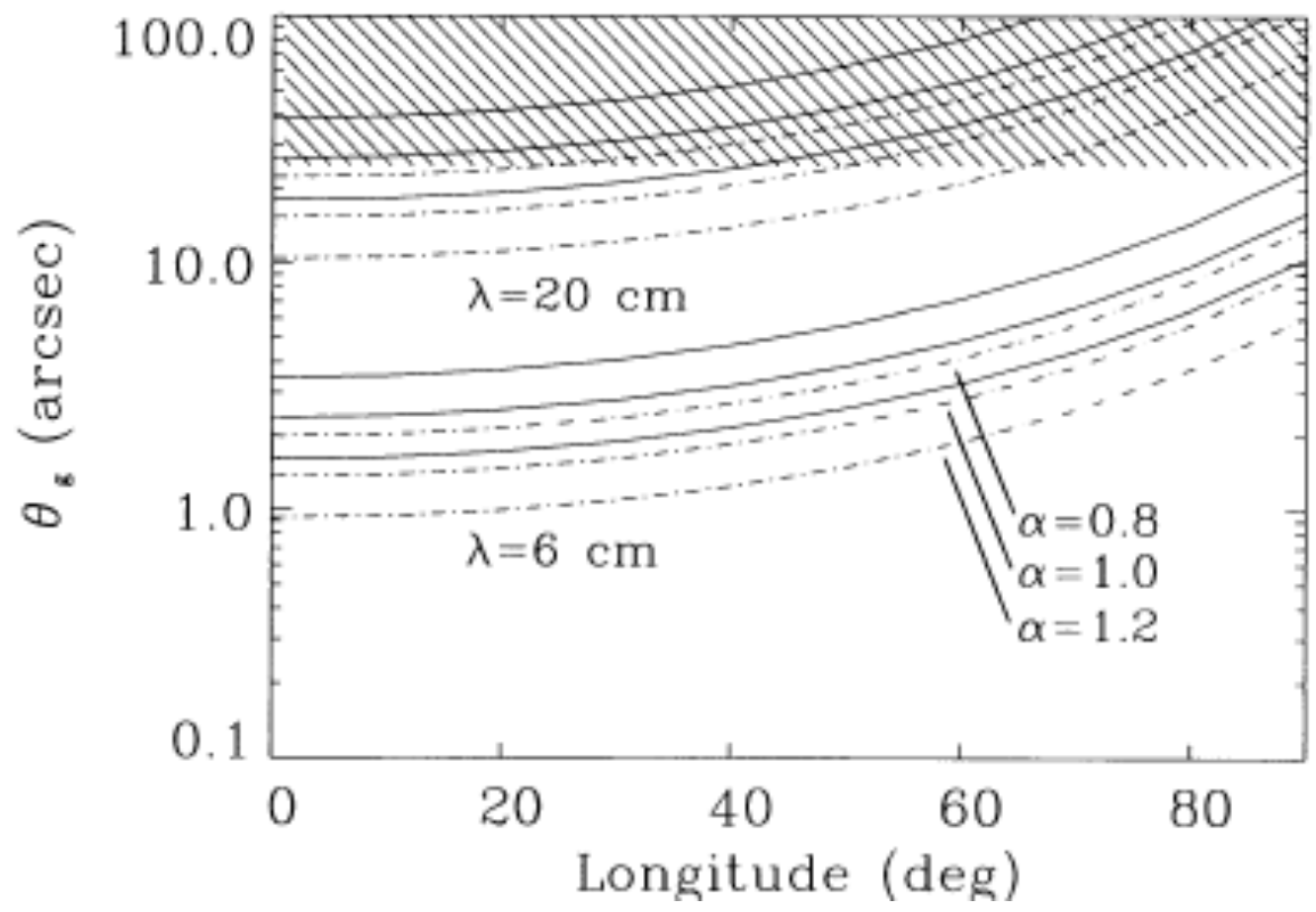
and when a turbulent medium lies between the source and the observer

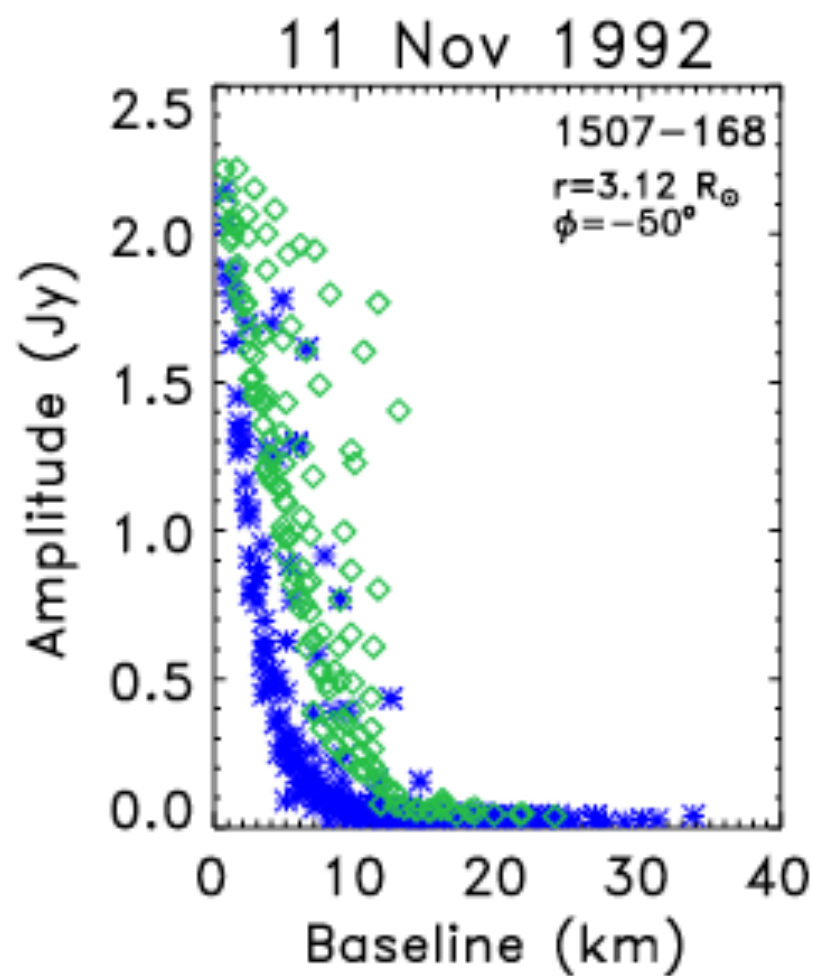
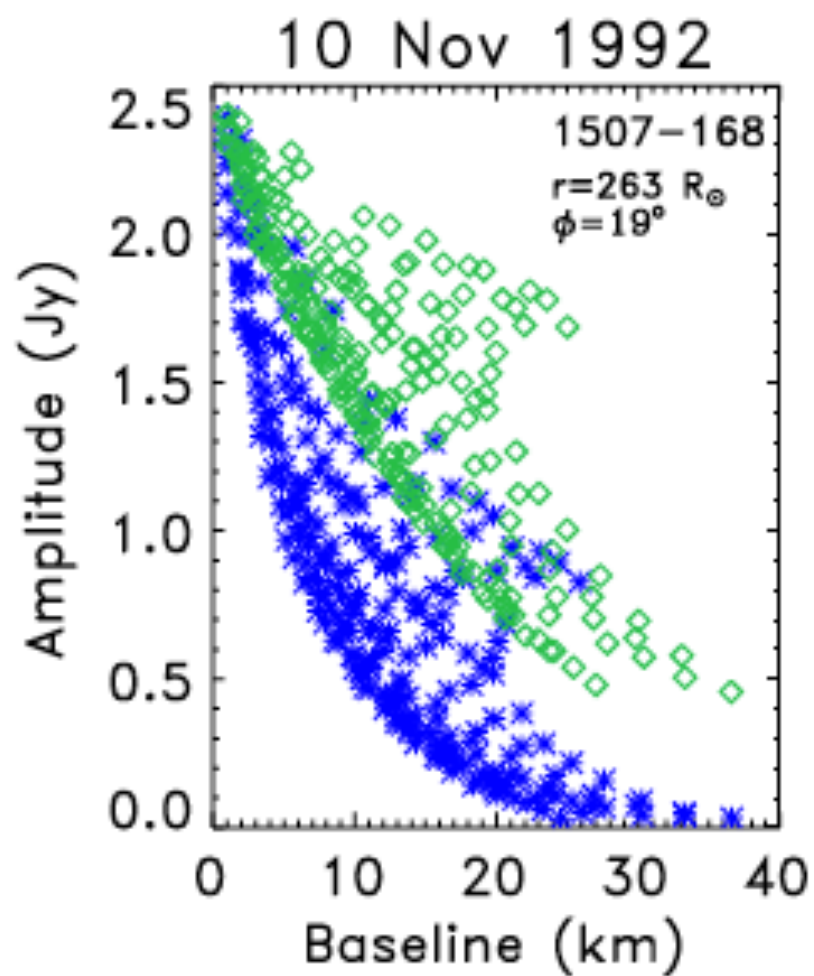
$$\Gamma(\mathbf{s}) = V(\mathbf{s}) \exp [-D(\mathbf{s})/2]$$

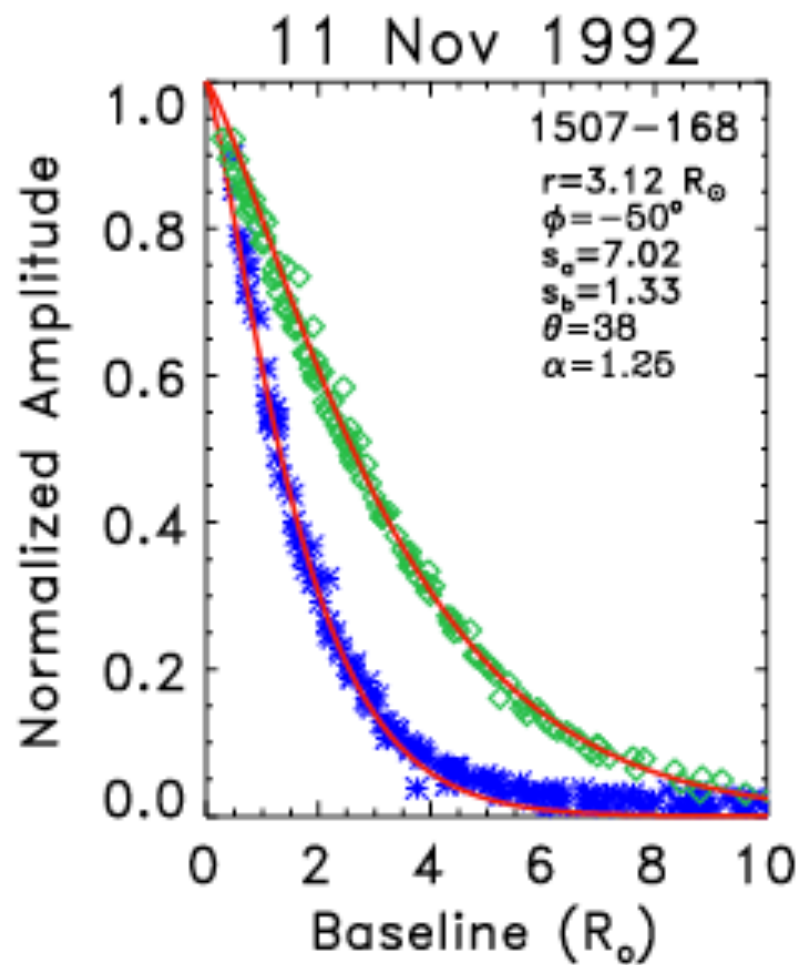
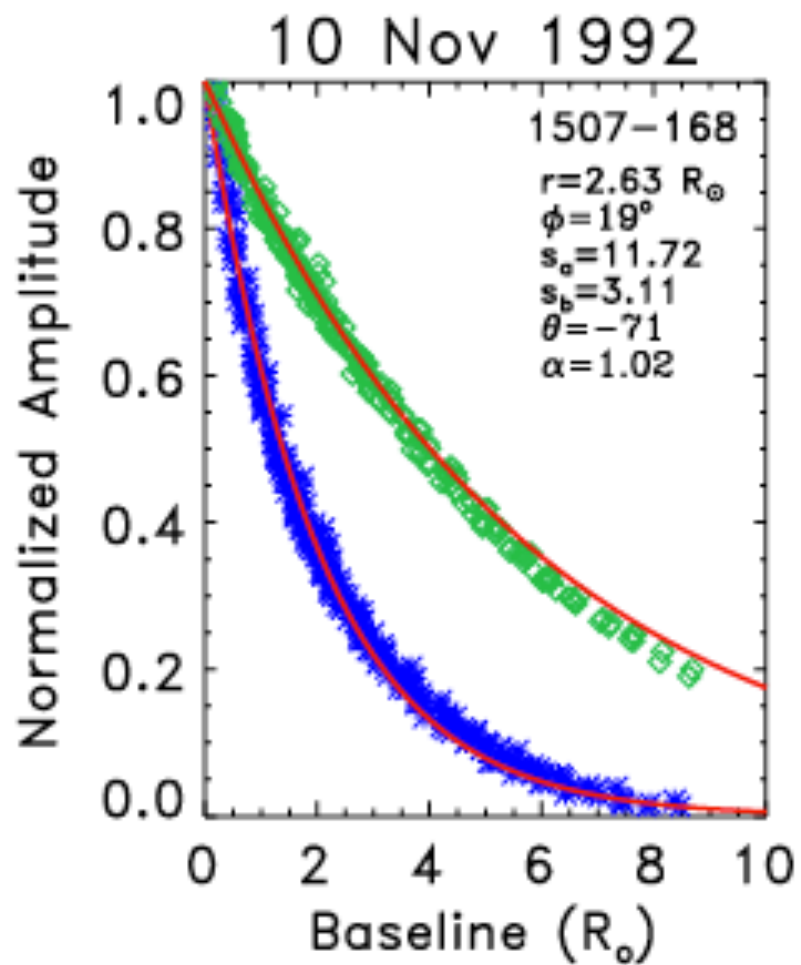
i.e, the image of the source is convolved with a Gaussian angular broadening function.



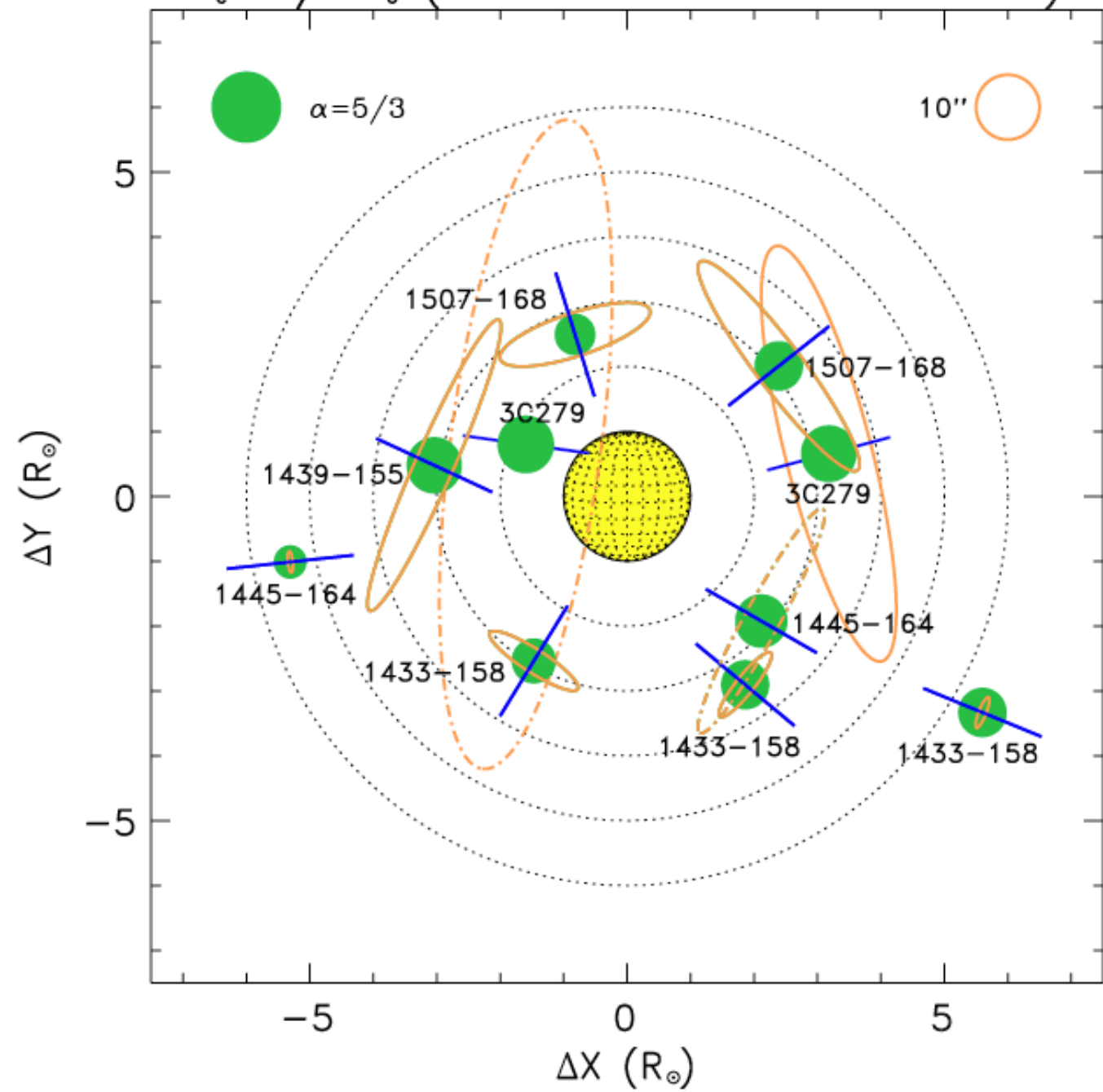




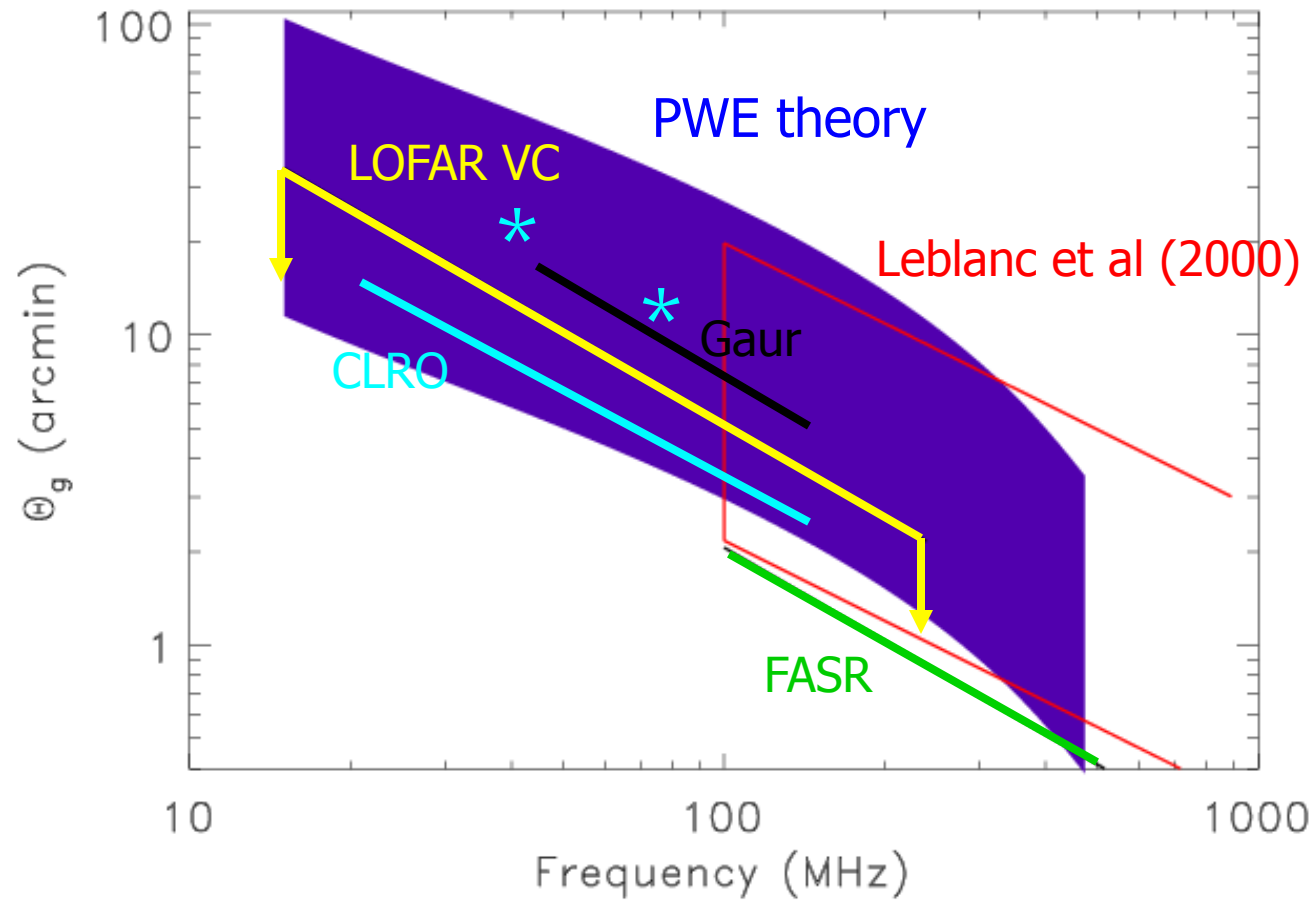


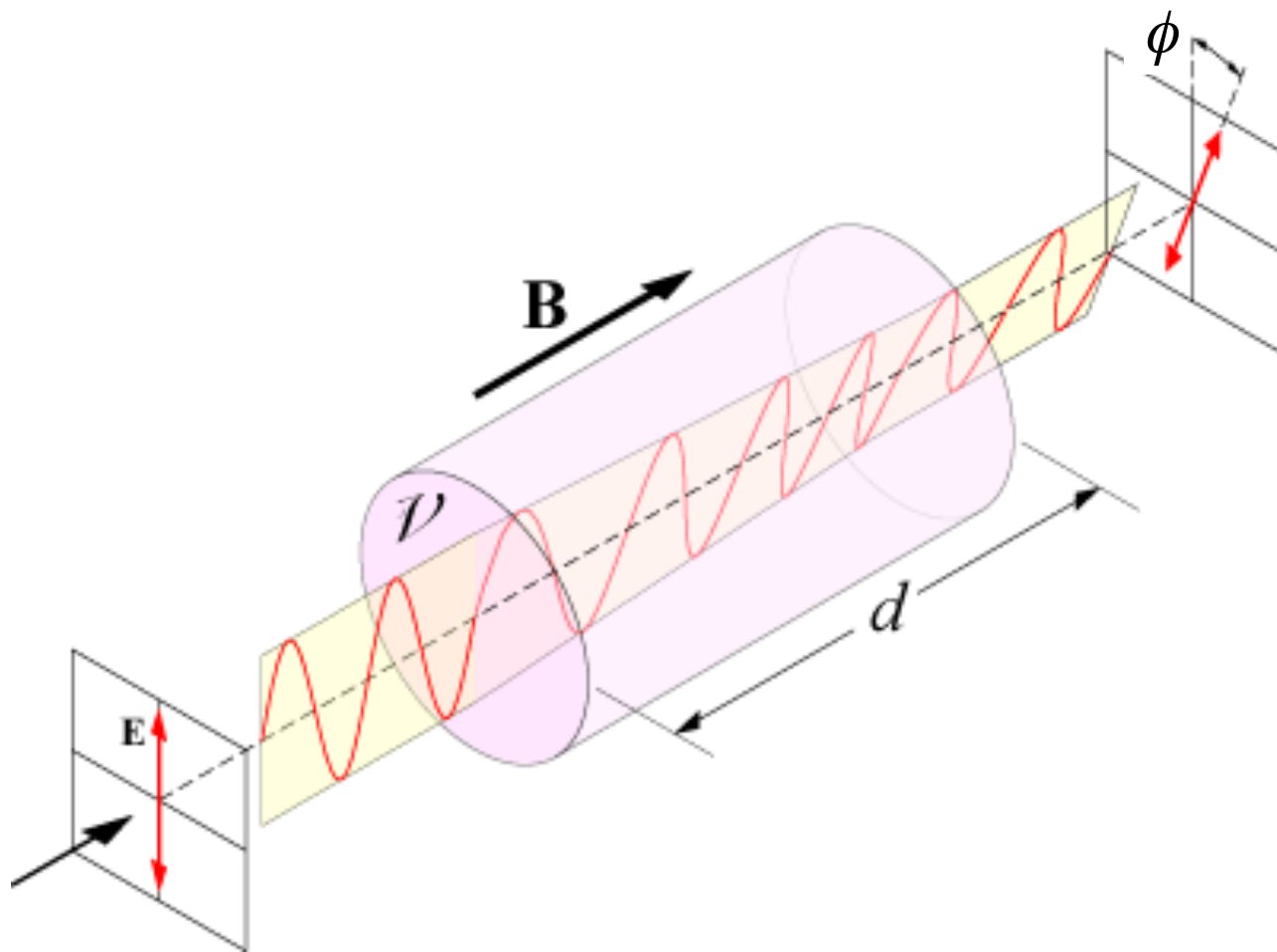


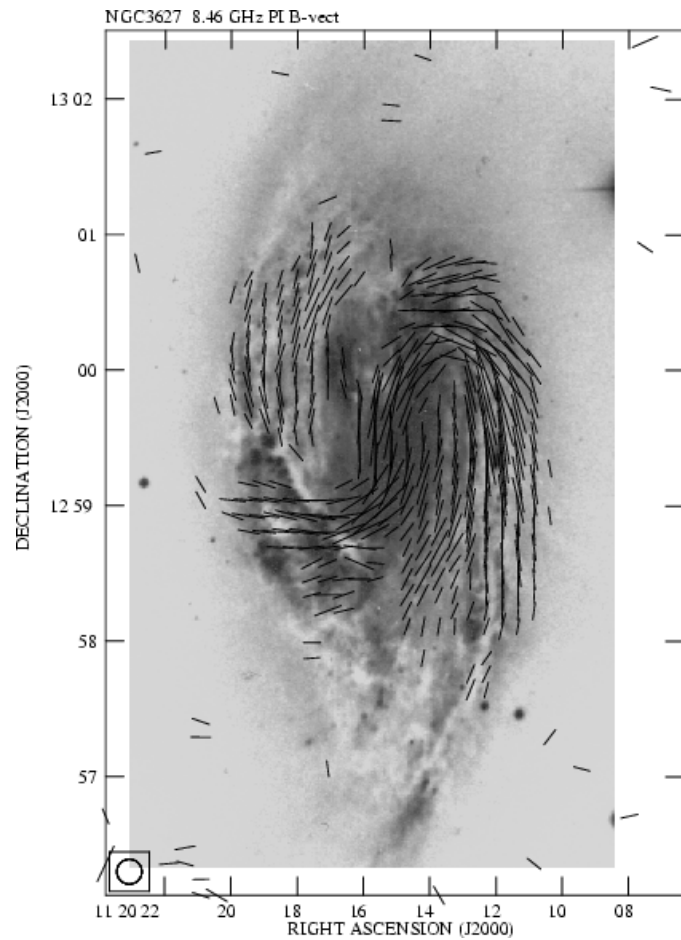
$\theta_c = 1/k_s$  (Normalized to  $\lambda = 20$  cm)



# Angular broadening of solar radio sources by coronal turbulence

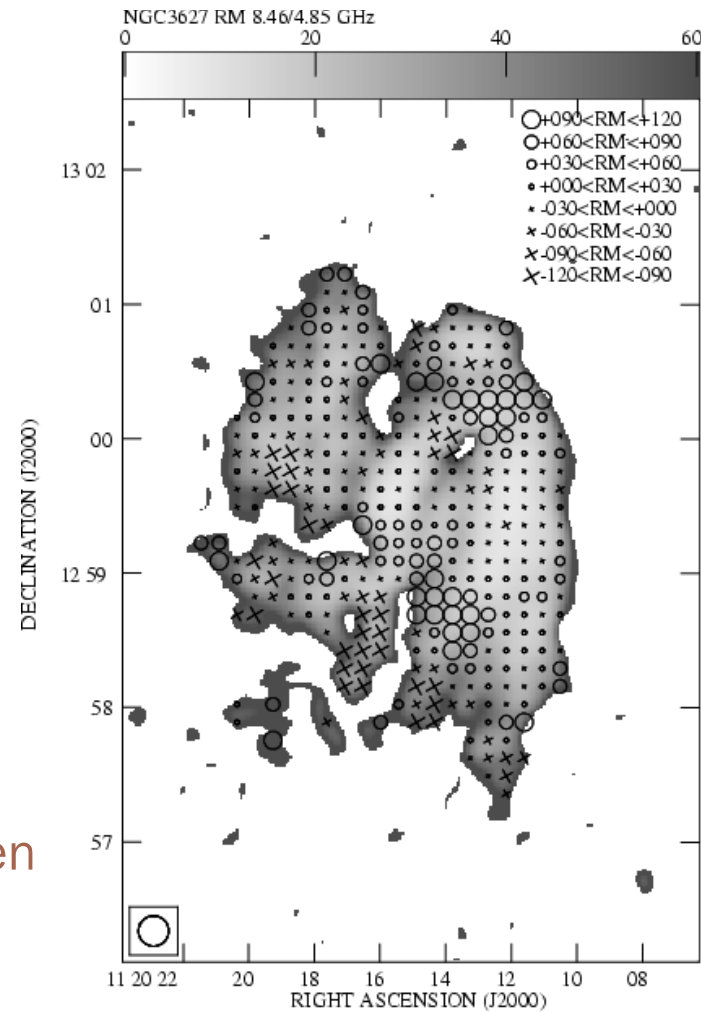




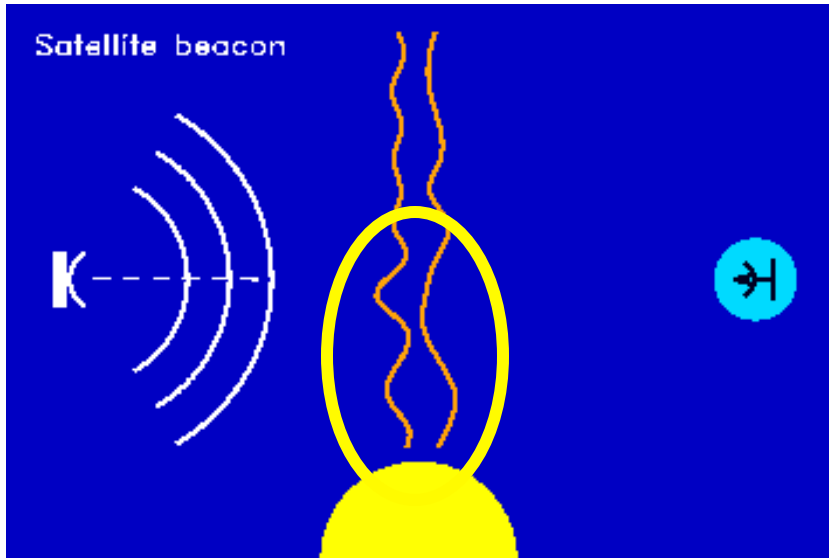


VLA 8.4 GHz map of NGC3627 with magnetic field vectors superposed.

Map of Faraday rotation between 8.4 and 4.9 GHz





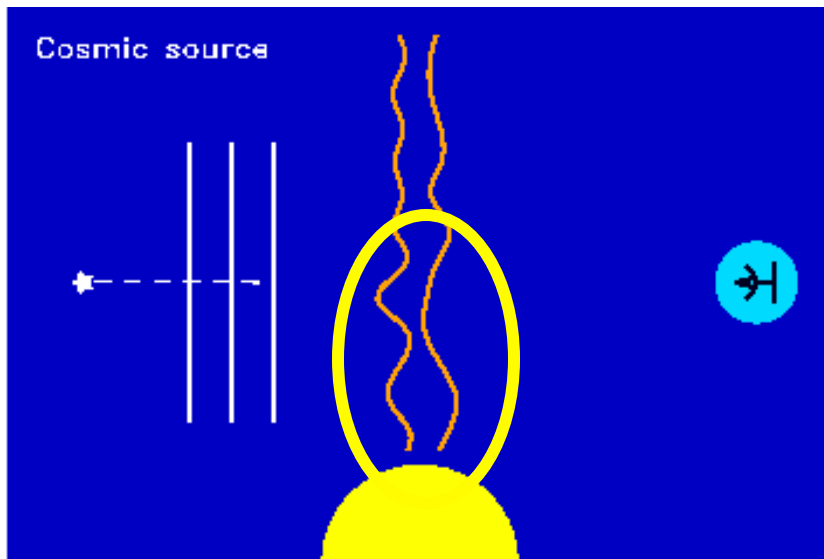


The position angle of a linearly polarized signal passing through a magnetized plasma is

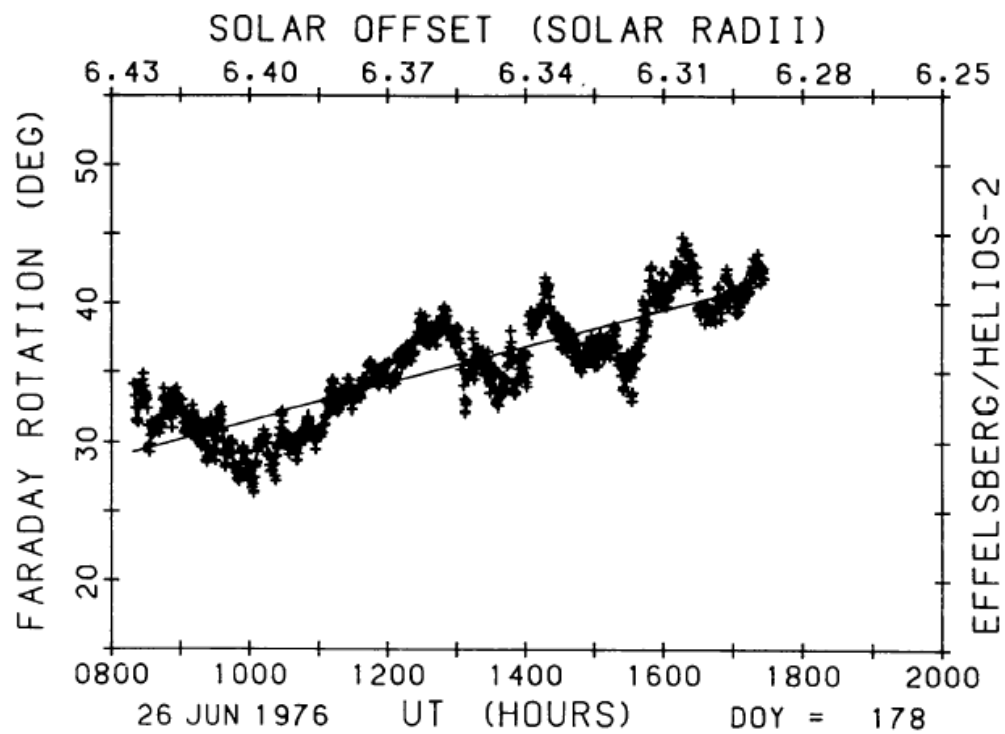
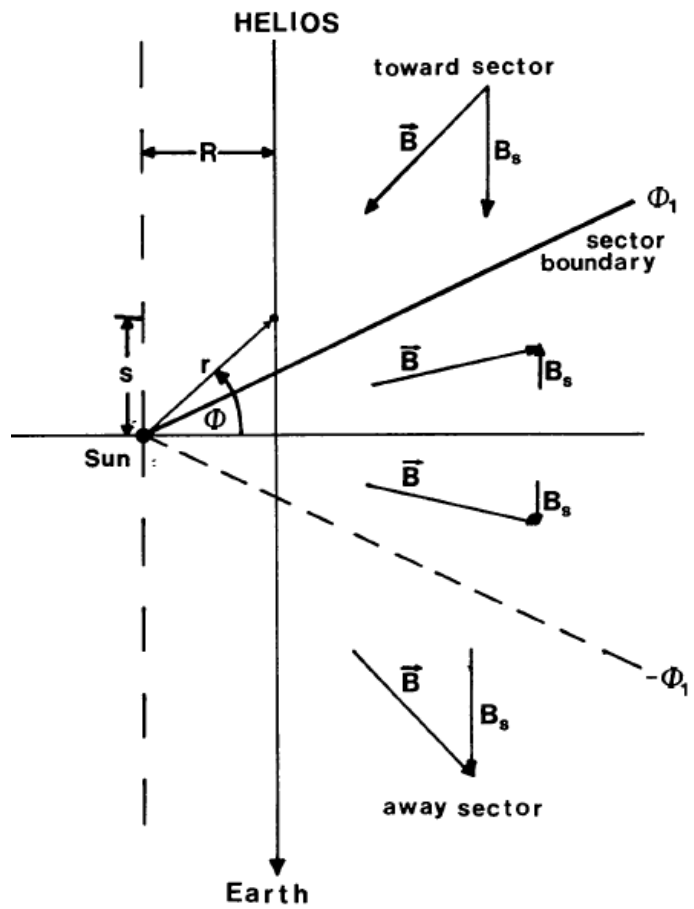
$$\phi \propto \lambda^2 \int n_e B_l ds$$

The passage of a transient (e.g., CME) perturbs the ambient electron number density and magnetic field -  $\phi$  is therefore also perturbed as

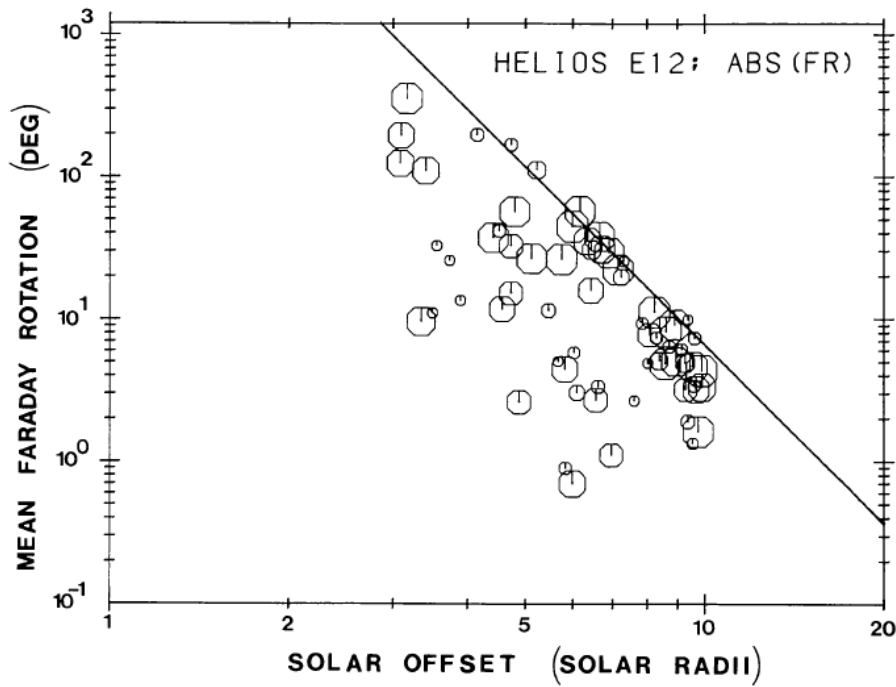
$$\Delta\phi \propto \lambda^2 \int n_e^{tr} B_l^{tr} ds$$



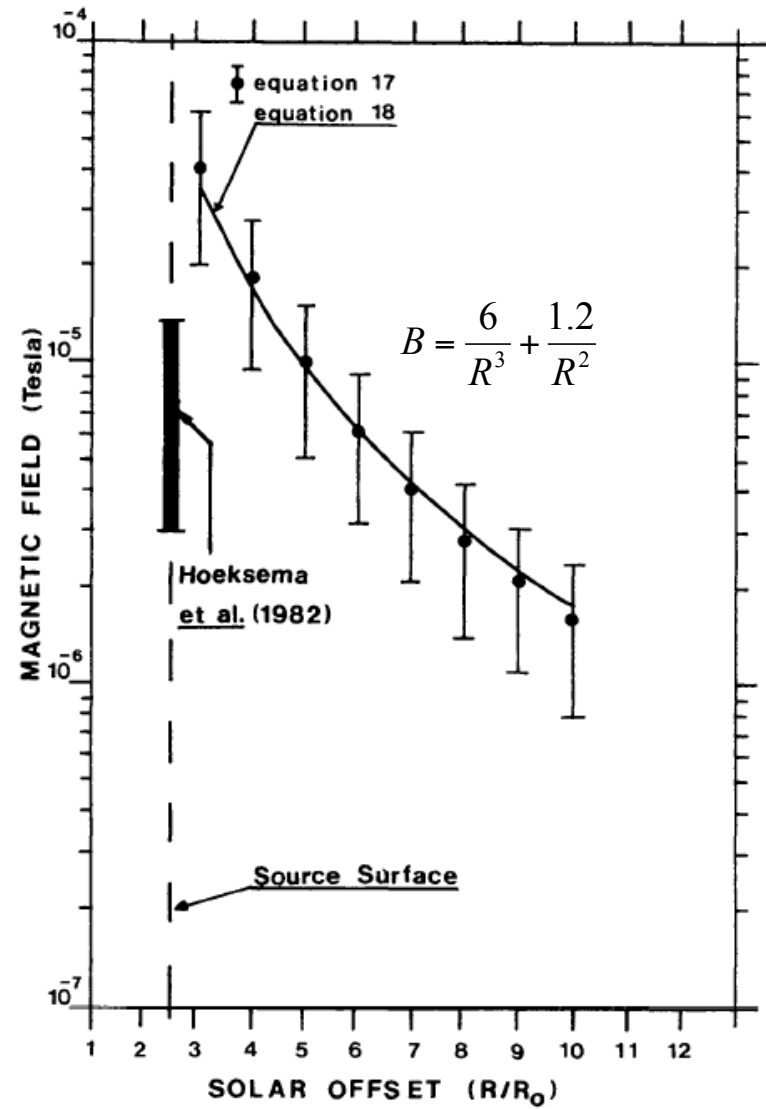
If an estimate of  $n_e^{CME}$  may be determined using white light coronagraphs, allowing an estimate of the mean longitudinal magnetic field to be derived.



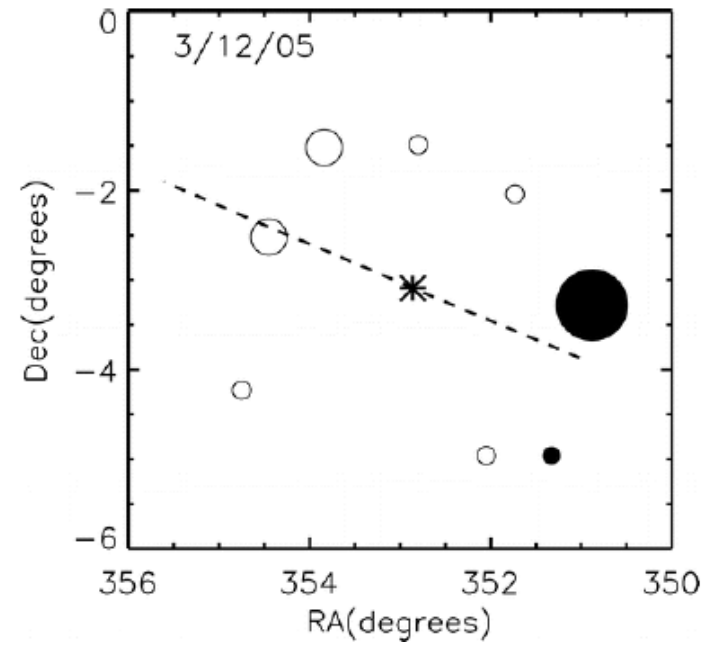
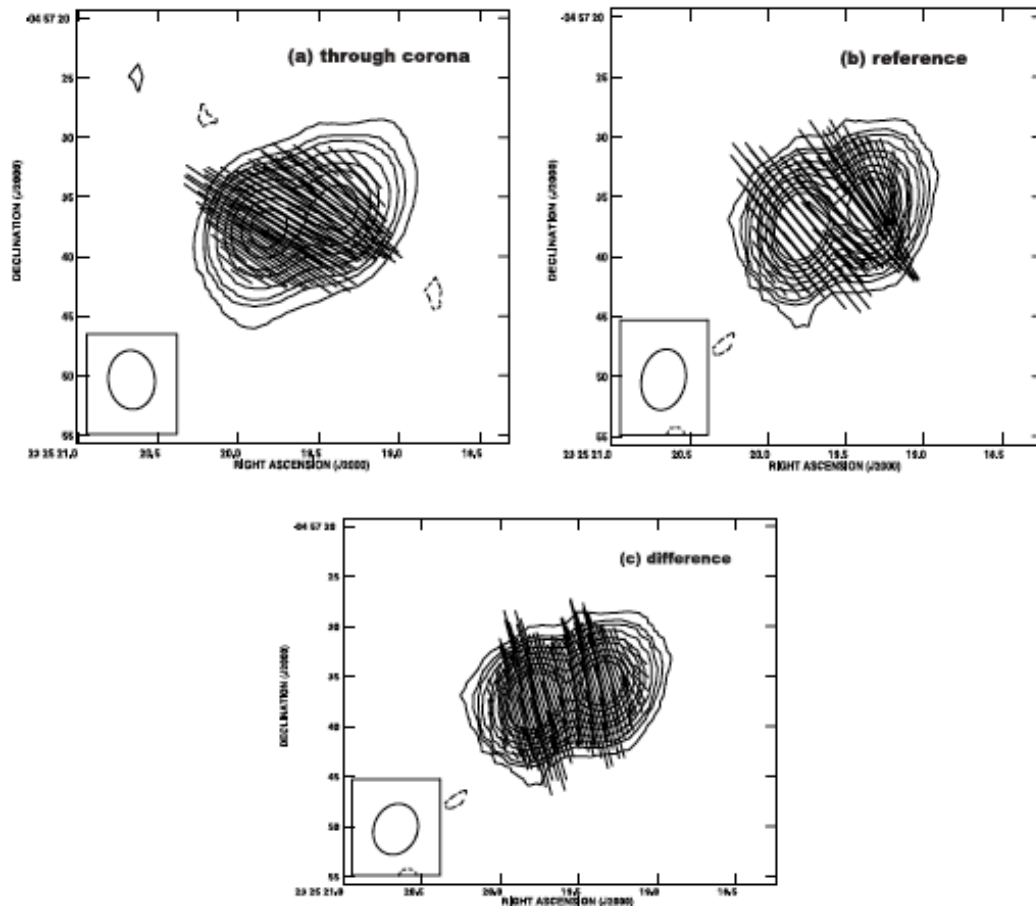
Patzöld et al. (1987)



Faraday rotation measurements using a radio beacon on Helios



Patzöld et al. (1987)



Forward fitting needed to disentangle B from  $n_e$ .

Ingleby et al 2007

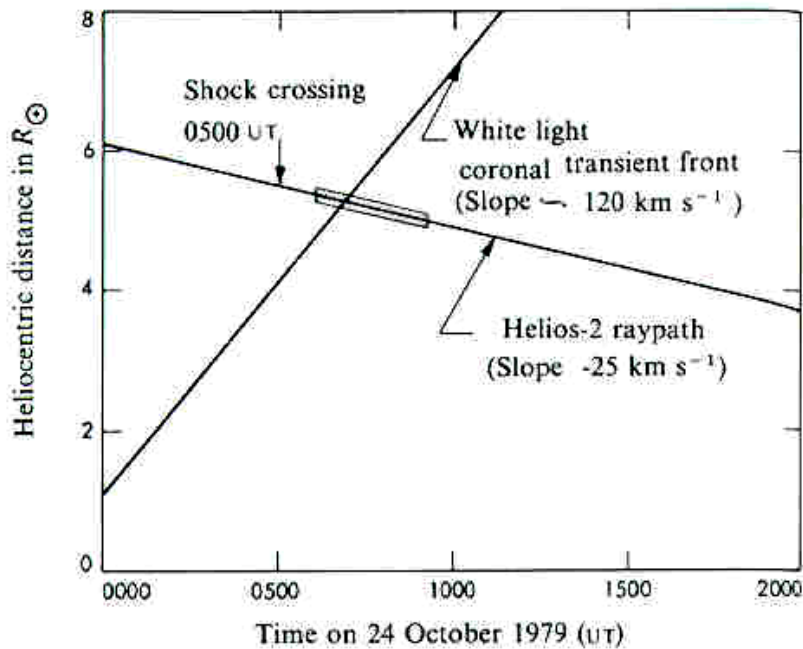


**Fig. 2** Height-time profiles for the Helios-2 raypath and Solwind white light coronal front measurements. The cross-hatched region indicates the possible range of intersections between the Helios-2 raypath and the white light transient front allowing for the  $120 \pm 120 \text{ km s}^{-1}$  uncertainty in the measured transient speed.

$$\Delta\nu \sim \sigma_{ne} V_p$$

from Woo *et al.* 1982

Observation of spectral broadening as a result of propagation through a CME.

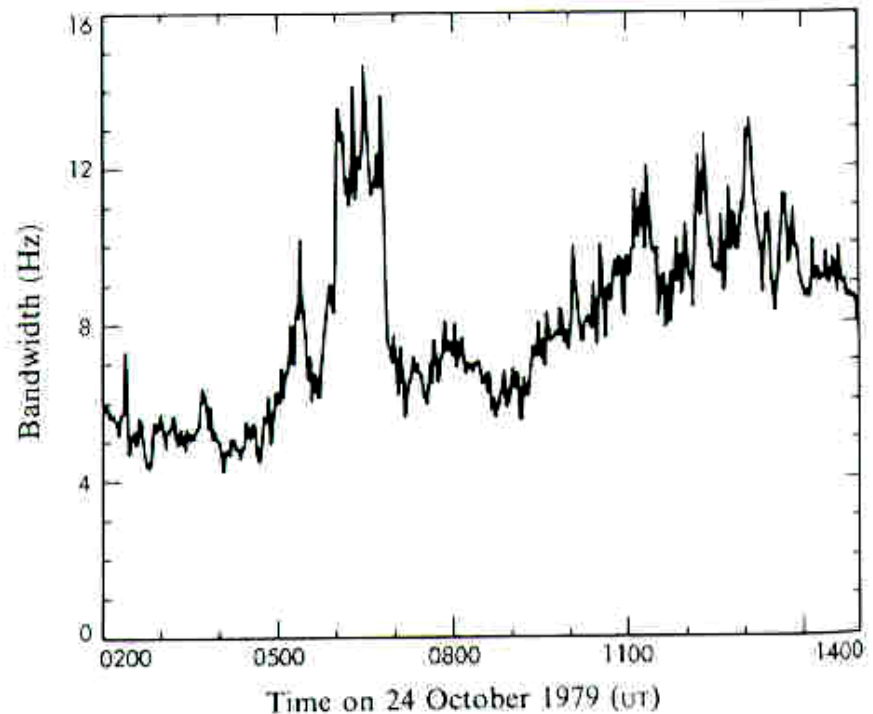
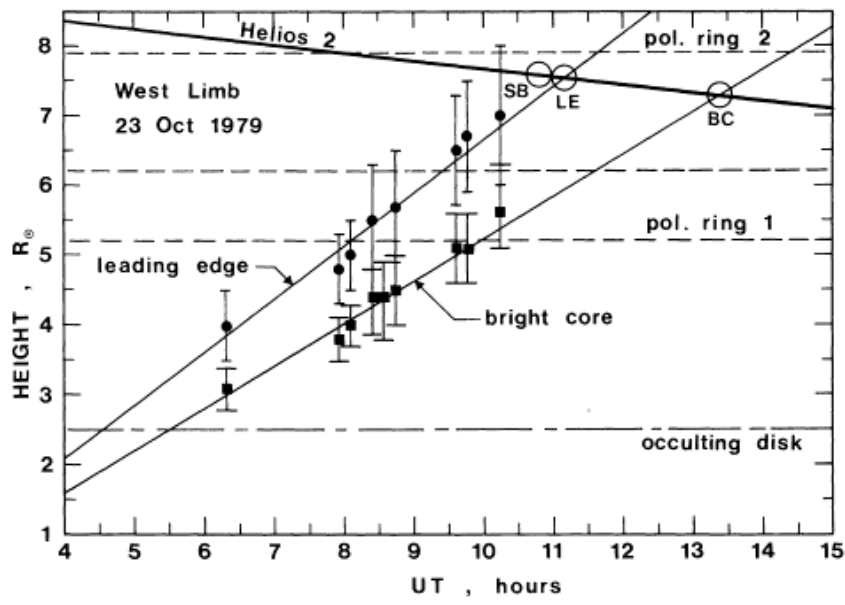
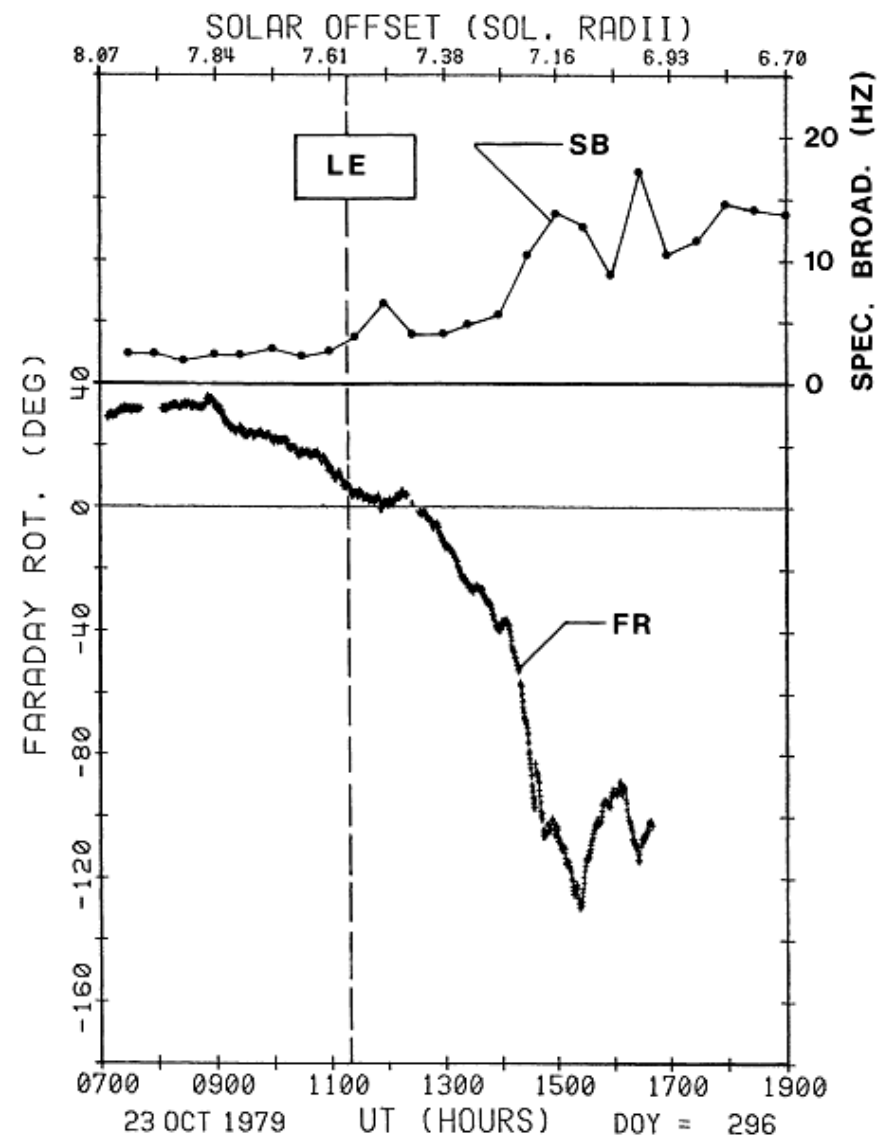


**Fig. 3** Time history of Helios-2 2.3-GHz spectral broadening bandwidth BW.



A total of 5 CMEs were observed. There was a one-to-one correspondence between SB and FR perturbations.

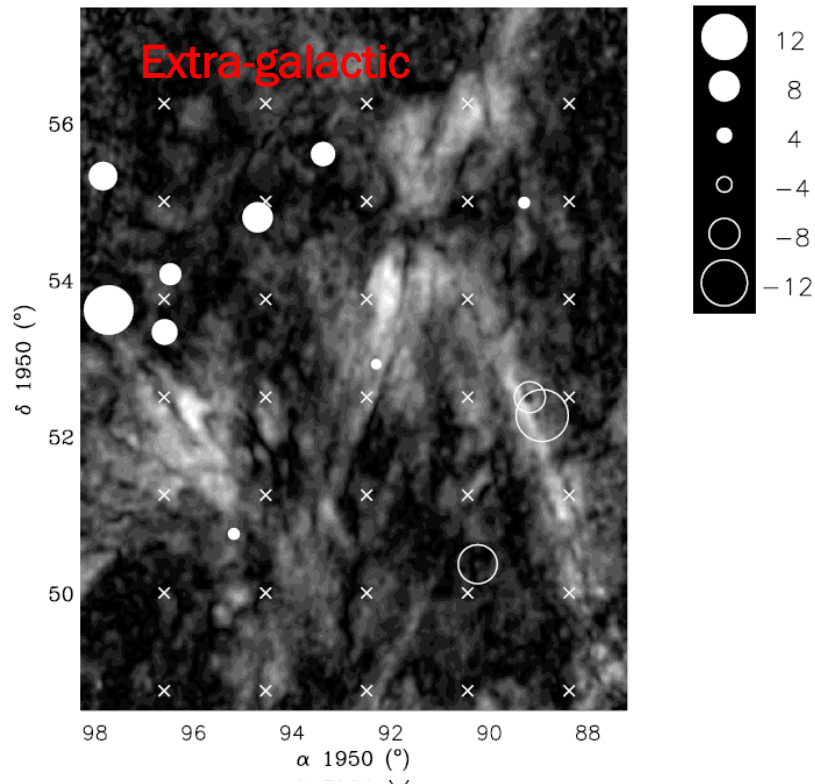
Mean longitudinal magnetic fields ranged between 10-100 mG, normalized to a radial distance of 2.5 solar radii.



# FR SOURCES

## HOW MANY SOURCES AT OUR FREQUENCIES?

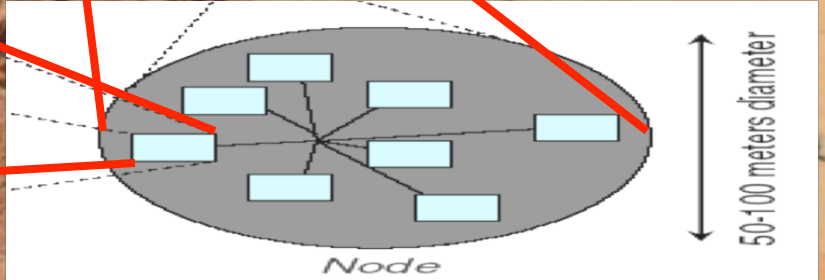
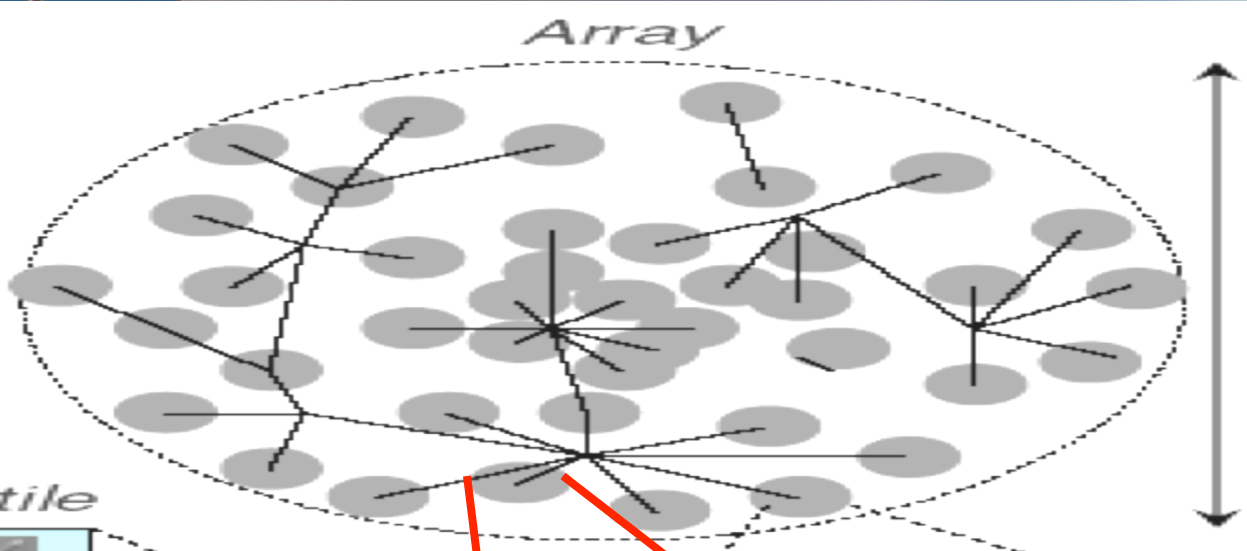
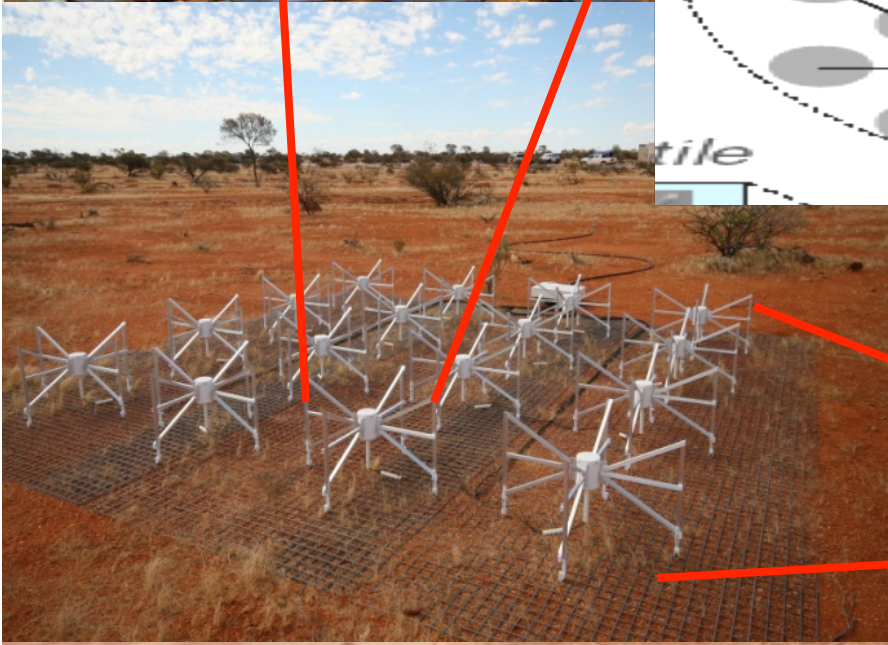
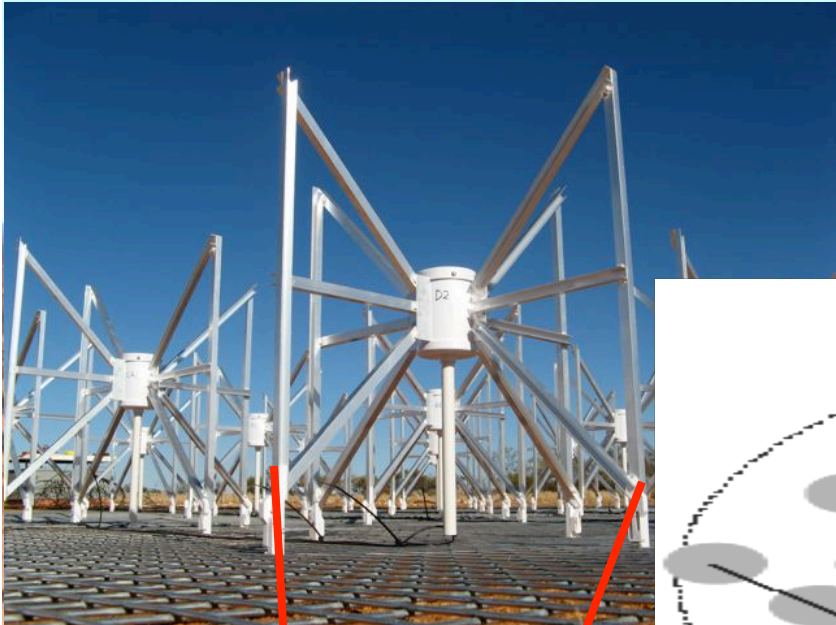
Near Auriga constellation



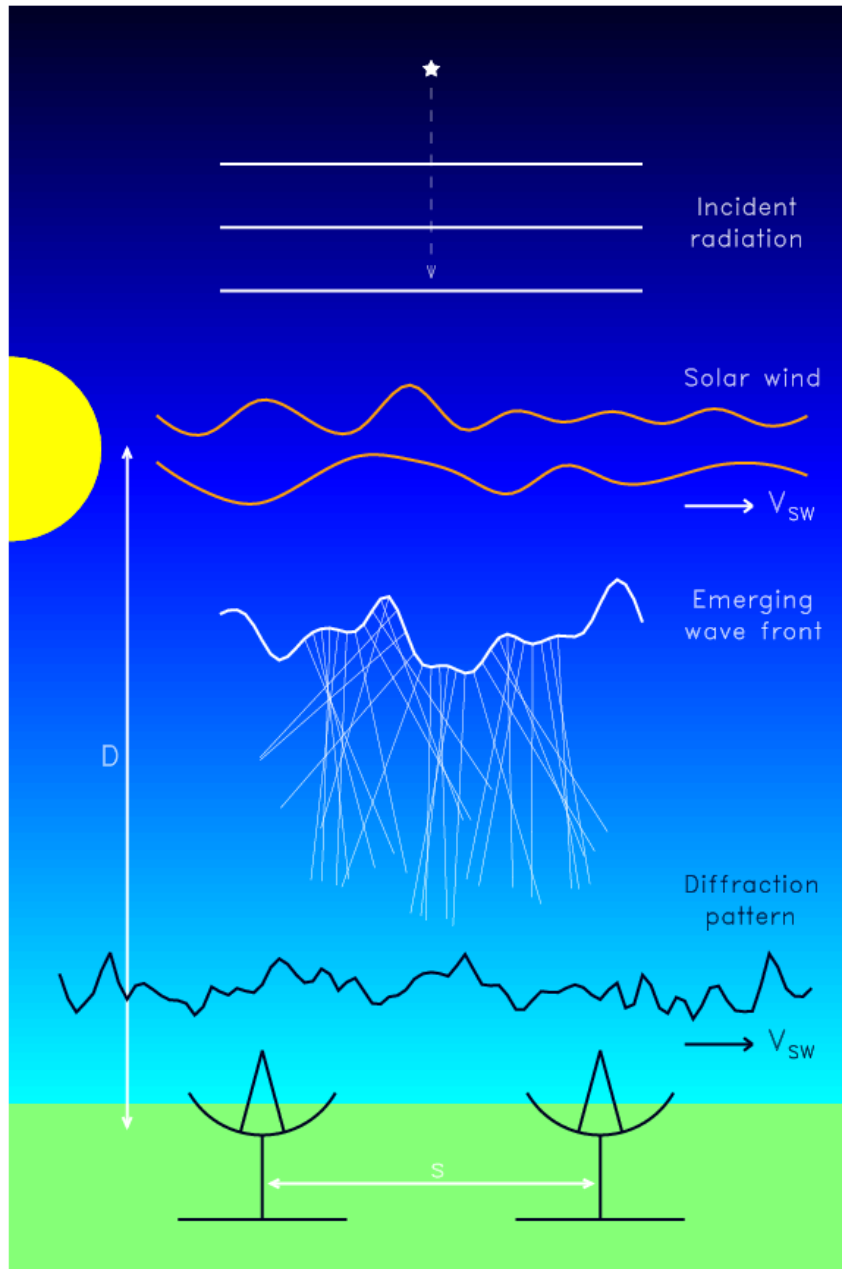
- ✘ Polarization tends to decrease with frequency
- ✘ Westerbork Northern Sky Survey at 327 MHz
- ✘ One extragalactic source ~ 2 square degrees
- ✘ RM of several hundred sources detectable in five minute integration
- ✘ Potential to use diffuse galactic emission as well

Haverkorn, 2003

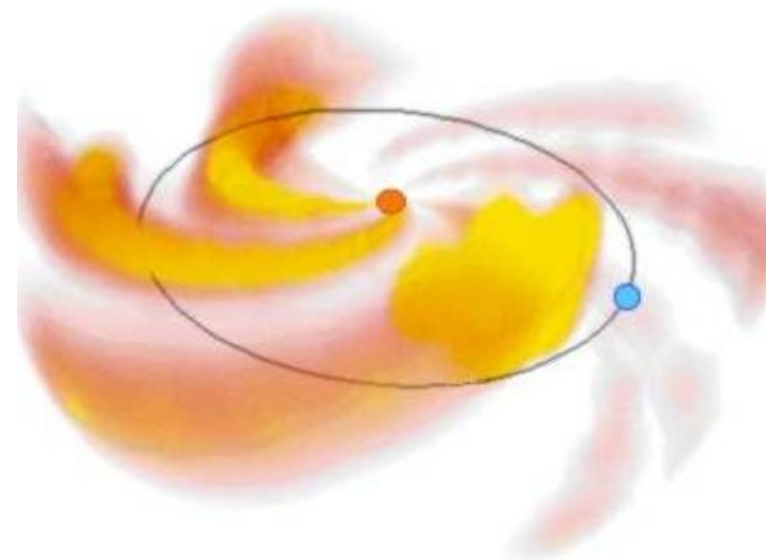
Currently building out from 32 tile demonstrator to 128 tiles







Tomographic reconstruction of recurrent structures in the inner heliosphere using observations of interplanetary scintillation (IPS).



LOFAR could provide much more comprehensive maps at higher angular resolution.

Jackson et al. 2001



